Animal Nutrition 19 (2024) 41–55

Contents lists available at ScienceDirect

Animal Nutrition

journal homepage: http://www.keaipublishing.com/en/journals/aninu/

Original Research Article

# Butyrate metabolism in rumen epithelium affected by host and diet regime through regulating microbiota in a goat model

Yimin Zhuang [a, b, c], Mahmoud M. Abdelsattar [b], Yuze Fu [b], Naifeng Zhang [b, *], Jianmin Chai [a, d, *]

[a] Guangdong Provincial Key Laboratory of Animal Molecular Design and Precise Breeding, College of Life Science and Engineering, Foshan University, Foshan 528225, China
[b] Key Laboratory of Feed Biotechnology of the Ministry of Agriculture and Rural Affairs, Institute of Feed Research of Chinese Academy of Agricultural Sciences, Beijing 100081, China
[c] State Key Laboratory of Animal Nutrition, College of Animal Science and Technology, China Agricultural University, Beijing 100193, China
[d] Division of Agriculture, Department of Animal Science, University of Arkansas, Fayetteville, AR 72701, USA

ARTICLE INFO

*Article history:*
Received 20 July 2023
Received in revised form
29 March 2024
Accepted 4 April 2024
Available online 24 July 2024

*Keywords:*
Rumen microbiota
Rumen epithelial development
Multi-omics
Host-microbe interaction

ABSTRACT

The rumen is an important organ that enables ruminants to digest nutrients. However, the biological mechanism by which the microbiota and its derived fatty acids regulate rumen development is still unclear. In this study, 18 female Haimen goats were selected and slaughtered at d 30, 60, and 90 of age. Multi-omics analyses (rumen microbial sequencing, host transcriptome sequencing, and rumen epithelial metabolomics) were performed to investigate host–microbe interactions from preweaning to postweaning in a goat model. With increasing age, and after the introduction of solid feed, the increased abundances of *Prevotella* and *Roseburia* showed positive correlations with volatile fatty acid (VFA) levels and morphological parameters ($P < 0.05$). Epithelial transcriptomic analysis showed that the expression levels of hub genes, including 3-hydroxy-3-methylglutaryl-CoA synthase isoform 2 (*HMGCS2*), enoyl-CoA hydratase, short chain 1 (*ECHS1*), and peroxisome proliferator activated receptor gamma (*PPARG*), were positively associated with animal phenotype ($P < 0.05$). These hub genes were mainly correlated to VFA metabolism, oxidative phosphorylation, and the mammalian target of rapamycin (mTOR) and peroxisome proliferator activated receptor (PPAR) signaling pathways ($P < 0.05$). Moreover, the primary metabolites in the epithelium changed from glucose preweaning to (R)-3-hydroxybutyric acid (BHBA) and acetoacetic acid (ACAC) postweaning ($P < 0.05$). Diet and butyrate were the major factors shaping epithelial metabolomics in young ruminants ($P < 0.05$). Multi-omics analysis showed that the rumen microbiota and VFA were mainly associated with the epithelial transcriptome, and that alterations in gene expression influenced host metabolism. The "butanoate metabolism" pathway, which transcriptomic and metabolomic analyses identified as being upregulated with age, produces ketones that regulate the "oxidative phosphorylation" pathway, which could provide energy for the development of rumen papillae. Our findings reveal the changes that occur in the rumen microbiota, host transcriptome, and metabolome with age, and validate the role of microbiota-derived VFA in manipulating host gene expression and subsequent metabolism. This study provides insight into the molecular mechanisms of host–microbe interactions in goats and supplies a theoretical basis and guidance for precise nutritional regulation during the critical time window for rumen development of young ruminants.


* Corresponding authors.
*E-mail addresses:* zhangnaifeng@caas.cn (N. Zhang), Jchai@fosu.edu.cn (J. Chai).
Peer review under the responsibility of Chinese Association of Animal Science and Veterinary Medicine.

Production and Hosting by Elsevier on behalf of KeAi

## 1. Introduction

The complex rumen microbial ecosystem and its relationship with the host is an excellent model for investigating host–microbe interactions (Furman et al., 2020; Mizrahi et al., 2021). The close dynamic interaction between the rumen

https://doi.org/10.1016/j.aninu.2024.04.027

epithelium maintains homeostasis and metabolism in the rumen, enabling ruminants to produce edible products and contribute to food security. The rumen is one of the most important digestive organs and, through its microbial community, converts dietary plant fiber and low-quality protein into volatile fatty acids (VFA), which supply 70% to 80% of the energy required for rumen development and host growth (Lv et al., 2019; Xue et al., 2020b). It is worth noting that the rumen epithelium is a major site of absorption of the VFA produced by the rumen microbiota. The rumen microbiome and epithelial function are not well developed in young ruminants. With increasing age and the introduction of solid feed, the rumen microbial community gradually matures and ferments more VFA, which stimulates synchronous growth and development of the rumen epithelium (Abdelsattar et al., 2022; Chai et al., 2021). However, the biological mechanism by which VFA regulate metabolic pathways during rumen epithelium development is still unclear, and our understanding of host–microbe interactions in the rumen remains incomplete.

Age, accompanied by dietary changes and weaning, significantly impacts the function and metabolism of the rumen (Chai et al., 2024b). From preweaning to postweaning, the rumen epithelial capacity to absorb, transport, and metabolize VFA changes dramatically (Malmuthuge et al., 2019). Generally, VFA derived from the microbiota are transferred across the rumen epithelial barrier via specific transporters or passive diffusion (Kirat et al., 2007; Yohe et al., 2019). Then, after entering rumen epithelial cells, they are metabolized into secondary metabolites, such as ketones. Finally, the end metabolites are transported into the blood, where they are available for use by the host. Most previous studies have investigated epithelial gene expression by transcriptome sequencing. For instance, with increasing age, the expression of genes related to cellular growth and proliferation, molecular transport, the cell cycle, and so on increases in the rumen epithelium (Baldwin Vi et al., 2021; Malmuthuge et al., 2019). In particular, acetyl-CoA acetyltransferase 1 (*ACAT1*), 3-hydroxybutyrate dehydrogenase 1 (*BDH1*), 3-hydroxy-3-methylglutaryl-CoA lyase (*HMGCL*), and 3-hydroxy-3-methylglutaryl-CoA synthase isoform 2 (*HMGCS2*) expression levels, which are associated with butanoate metabolism, ketogenic biosynthesis, pyruvate metabolism, as well as the tricarboxylic acid (TCA) cycle, are synchronized with rumen development (Naeem et al., 2012; Sun et al., 2021; Wang et al., 2016; Zhang et al., 2022; Zhuang et al., 2023a). Although the above studies have shown that changes in both age and diet significantly alter rumen epithelium gene expression, it remains unclear whether age or diet is the most important factor promoting rumen development in young ruminants. Furthermore, to date there have been few reports of transcriptomic changes in the goat epithelium from preweaning to postweaning that could reflect alterations in the rumen microbiota and VFA production. Moreover, studies of the associations among host metabolites, rumen epithelium gene expression, and alterations in molecular pathways during growth and development are still lacking. Additionally, complex host–microbe interactions in the rumen still need to be clarified.

We hypothesized that the changes that occur in the goat rumen microbiota and VFA production with increasing age influence epithelial gene expression and metabolism, as well as rumen development. Thus, in this study, we employed multi-omics (16S sequencing to assess the rumen microbiota and transcriptomics and metabolomics analyses of the rumen epithelium) with an integrated bioinformatics approach to comprehensively explore host–microbe interactions and their roles in rumen development in goat kids from the suckling period to postweaning. Furthermore, we analyzed the signaling and metabolic pathways associated with VFA production and epithelial morphology. The detailed description of the molecular mechanisms underlying host–microbe interactions in the rumen presented here may provide new insights into how to modulate rumen development and improve ruminant productivity and health to meet global food demands.

## 2. Materials and methods

### 2.1. Animal ethics statement

The study was approved by the Animal Ethics Committee of the Chinese Academy of Agricultural Sciences (approval number: AEC-CAAS-20200605; approval date: 5 June 2020).

### 2.2. Animals and experimental design

A total of 18 healthy, female, 30-d-old Haimen goat kids weighing 5.79 ± 0.28 kg were included in this study. Six randomly selected goat kids were weighed and humanely euthanized at d 30, 60, and 90, respectively, for sample collection. From birth to d 30, all the goat kids lived with their dams and consumed breast milk as their only food source. Beginning on d 30, the goat kids were also given solid feed (nutrient content shown in Table S1). Subsequently, each goat was weaned off breast milk at d 60 and moved into a separate pen for raising to d 90. From d 30 to 90, the goat kids had ad libitum access to water and solid feed, and their feed intakes were recorded daily. During the experimental period, the feed was refreshed every day, and the sheepfold was cleaned regularly to ensure that the feed did not deteriorate and that the living environment was tidy. Ambient noise and the number of people who had access to the goats were also strictly controlled to avoid provoking fear and stress in the goats. Veterinarians monitored the goats' physiology and wellbeing daily to ensure that they were healthy.

### 2.3. Collection of rumen contents and rumen epithelial tissue

After each goat was euthanized, its abdominal cavity was opened immediately, and the whole rumen was removed. A small incision was made in the ventral sac with a scalpel, and the rumen digesta (approximately 8 mL per animal) was quickly collected with a sterile beaker. The collected rumen digesta was mixed thoroughly, divided into four, 2-mL aliquots, and stored at −80 °C in cryopreservation tubes for subsequent sequencing. Following this, 10 mL of rumen fluid was filtered from the remaining digesta through four layers of gauze, placed in a 15-mL centrifuge tube, and immediately frozen at −20 °C for later analysis of rumen fermentation parameters.

Rumen epithelium samples from the bottom of the ventral sac were collected within 10 min of euthanasia. Each epithelium sample (approximately 10 $cm^2$) was washed with bacteria-free PBS (pH = 7) to remove residue from the gaps between the papillae. A 2 cm × 2 cm section of the tissue sample (approximately 4 $cm^2$) was fixed in a 250-mL jar containing 10% neutral formalin solution to detect epithelial morphology. The remaining epithelial tissue was divided into two equal parts, snap frozen in liquid nitrogen, and stored at −80 °C for epithelial transcriptomics and metabolomics.

### 2.4. Starter feed nutrient composition analysis

The nutrient composition of the starter feed was analyzed using Association of Official Analytical Chemists (AOAC) methods (AOAC, 2000). Specifically, starter samples were thawed overnight at room temperature and dried in an oven at 65 °C for 48 h. Then, the

samples were ground, passed through a 1-mm sieve, and dried in an oven at 135 °C for 2 h (method 930.15; AOAC, 2000) to measure the dry matter (DM) content. The ash content was determined after the samples were heated at 600 °C for 6 h in a muffle furnace (SGM M12-12, SIGMA Co., Ltd., Luoyang, China) (method 924.05; AOAC, 2000). The total nitrogen content of the starter samples was measured using an Auto-Analyzer (Kjeltec sampler 8420, FOSS Co., Ltd., Hillerod, Denmark) after Kjeldahl digestion (method 950.36; AOAC, 2000), and the crude protein (CP) content was calculated using the following formula: 6.25 × N. The ether extract (EE) content was defined as the DM weight loss after extraction with diethyl ether in a Soxhlet extraction apparatus for 8 h (method 920.39; AOAC, 2000). The neutral detergent fiber (NDF) and acid detergent fiber (ADF) contents were measured using an ANKOM fiber analyzer (A2000i, American ANKOM, Macedon, NY, USA) (Van Soest et al., 1991). Ca and P contents were determined using an atomic absorption spectrometer (AAnalyst 300, PerkinElmer Inc., Boston, USA) (method 968.08; AOAC, 2000) after wet-ash digestion with nitric and perchloric acid (method 935.13; AOAC, 2000).

### 2.5. Determination of rumen fermentation parameters and morphology

The rumen fluid samples were thawed at 4 °C and then centrifuged at 2500 × *g* at room temperature. Next, 1 mL of the supernatant per sample was transferred to a 1.5-mL centrifuge tube containing 0.2 mL of metaphosphoric acid solution (25%, w/v), cooled in an ice water bath at 4 °C for 30 min, and centrifuged at 10,000 × *g* at 4 °C. The resulting supernatant was collected and stored at 4 °C for subsequent analysis. The VFA concentration was detected using gas chromatography (GC - 6800, Beijing Beifen Tianpu Instrument Technology, Co., Ltd., Beijing, China).

Rumen epithelium tissue samples were dehydrated in an ethanol gradient, embedded in paraffin, and sliced into 6-μm sections. The sections were then stained with Yi-hong-hematoxylin (H.E.), and the rumen papilla structure was observed under a light microscope at a magnification of 40 × 10 times (Olympus BX-51, Olympus Corporation, Tokyo, Japan). An Image-Pro Express image analysis processing system (Image-Pro Plus 6.0, Media Cybernetics, Silver Spring, MD, USA) was used to observe and measure the rumen papilla length, papilla width, lamina propria thickness, and epithelial thickness. Three images of the rumen epithelium from each goat were analyzed.

### 2.6. Rumen microbiota DNA extraction, 16S rRNA sequencing, and bioinformatics analysis

A DNeasy PowerSoil Kit (Qiagen, Valencia, CA, USA) was used to extract microbial DNA from the rumen content samples. DNA quality was checked using a Thermo NanoDrop 2000 UV microphotometer and 1% agarose gel electrophoresis. The V3–V4 region was amplified using adaptor-linked universal primers (341F: 5'-CCTACGGGRSGCAGCAG-3'; 806R: 5'-GGACTACVVGGGTATCTAATC-3') (Lin et al., 2019). Using diluted genomic DNA as a template, PCR was performed using the high-fidelity enzyme from the KAPA HiFi Hotstart ReadyMix PCR kit to ensure the accuracy and efficiency of the amplification. The PCR products were run on an agarose gel and purified using an AxyPrep DNA Gel Recovery kit (AXYGEN Inc., Union City, CA, USA). To rule out contamination from reagents, negative controls for DNA extraction and PCR amplification were included, and no PCR products from the negative controls were detected on the agarose gel. The quality of the amplified DNA library was checked using a Thermo NanoDrop 2000 UV microphotometer and 2% agarose gel electrophoresis. A Qubit 2.0 Fluorometer (Thermo Fisher Scientific, Waltham, MA, USA) was used to quantify the library. Amplicon libraries were sequenced using an Illumina Miseq PE250 platform (Realbio Technology Genomics Institute, Shanghai, China).

Mothur software (version 1.39.1) (Kozich et al., 2013) was used to process the raw sequences. Using the MiSeq SOP (https://mothur.org/wiki/miseq_sop), contigs merge, quality-filtering, alignment to the SILVA (v132) database, and clustering into operational taxonomic units (OTU) at the level of 97% similarity were carried out. High-quality reads were identified by comparison to the RDP (Ribosomal Database Project) database (Cole et al., 2009).

### 2.7. Transcriptomic sequencing and analysis of the rumen epithelium

A total of 18 rumen epithelium samples were collected after slaughter and used for transcriptomic analysis. Total RNA from the rumen epithelial tissue was extracted using TRIzol reagent according to the manufacturer's protocol (Invitrogen, CA, USA). To ensure the RNA concentration and quality, the absorbed optical density ratio of total RNA (OD260/280 between 1.80 and 2.10) was measured using a NanoDrop ND-1000 spectrophotometer (Thermo Fisher Scientific, Madison, WI, USA), and RNA integrity was confirmed by running the samples on a 1.4% agarose-formaldehyde gel.

DNase I was used to eliminate double-stranded and single-stranded DNA contaminants from all RNA samples, and mRNA molecules were purified from total RNA using oligo (dT)-attached magnetic beads. After fragmenting the mRNA of samples into small pieces using a fragmentation reagent, first-strand cDNA was generated using random hexamer–primed reverse transcription, followed by second-strand cDNA synthesis. The synthesized cDNA was subjected to end-repair and then was 3′-adenylated. Adaptors were ligated to the ends of these 3′-adenylated cDNA fragments. The ligated products were amplified by PCR with specific primers. The PCR products were thermally denatured into a single strand, and then the single-stranded DNA molecules were cyclized with a single-segment bridge primer to obtain a single-strand cyclic DNA library using a BGISEQ-500 platform (The Beijing Genomics Institute, Shenzhen, China). The quality of the constructed library was verified, and then sequencing was carried out. The RNA library was sequenced at Beijing Genomics Institute (BGI) Co., Ltd. A Pacbio RS II sequencer (Pacific Biosciences, CA, USA) was used to obtain 150-bp paired-end reads, according to the manufacturer's instructions.

After quality control of raw reads, HISAT2 was used to align the clean reads to the host genome. StringTie (version 1.3.4d) was used to map reads to describe the expression levels of the gene transcripts. Then, we used the fragments per kilobase of transcript per million fragments mapped (FPKM) method to calculate gene expression levels. Differentially expressed genes (DEGs) were identified by the DESeq method, with the following threshold values: $\log_2$ (fold change) $\geq 1$ and $P < 0.05$. Only genes whose expression levels were above the detection threshold (FPKM > 0.1 for each sample) were subjected to further analysis. Gene Ontology (GO) enrichment and Kyoto Encyclopedia of Genes and Genomes (KEGG) pathway analyses were carried out using KOBAS (version 3.0).

### 2.8. Rumen epithelium metabolite identification and quantification

The metabolites in the 18 rumen epithelium samples were measured using non-targeted metabolomics technology. In total, 100 mg of each sample was ground to a powder using a SCIENTZ-48 tissue grinder (SCIENTZ, Ningbo, China). Then, the rumen powder was transferred to a 5-mL tube and mixed with 2 mL of tissue extraction fluid (75% methanol and 25% dd$H_2O$) and three steel

beads. The mixture was ultra-sonicated at room temperature for 30 min and chilled on ice for 1 h, then centrifuged at 4 °C for 20 min at 6,000 × *g*. The supernatants were then transferred into 2-mL centrifuge tubes and vacuum-dried. The resulting samples were dissolved in 200 μL of 2-chlorobenzalanine (4 mg/L) 50% acetonitrile solution each, and the supernatants were passed through 0.22-μm filters. A quality control sample was generated by mixing equal volumes (20 μL) from each sample to calibrate the results. The remaining samples were subjected to LC-MS detection using a Thermo Q Exactive Plus (Thermo Fisher Scientific, Waltham, MA, USA) and a Thermo Vanquish (Thermo Fisher Scientific, Waltham, MA, USA) to detect the metabolites.

### 2.9. Statistical analyses

One-way ANOVA, performed using SPSS 19.0 (SPSS Inc., Chicago, IL, USA), was used to identify differences in rumen fermentation parameters and rumen epithelial morphology. Bar charts were created using GraphPad 8.0 software. Alpha diversity (Shannon and Chao1 indices) among the groups was assessed using the Kruskal–Wallis test and post hoc Dunn Kruskal–Wallis multiple comparison with Bonferroni correction. Beta diversity based on Bray–Curtis distances was assessed by analysis of similarity (ANOSIM). The diversity analysis outputs were visualized using the "ggplot2" package in R (version 3.6.0).

Multiple co-inertia analysis (MCIA) was performed using the R 'omicade4' package (v1.26.0) to detect general associations among the rumen microbiota, host transcriptome, and rumen epithelial metabolomics based on a custom script (Meng et al., 2014). Procrustes analysis of pair-wise omics datasets was performed using Tutools (http://www.cloudtutu.com), a free online data analysis website. Procrustes analysis was performed as follows: 1) the dimensionality of the original data was reduced; 2) based on the dimensionality reduction result distribution map, we superimposed the sample distribution of two groups of academic data in the same low-dimensional space and calculated the sum of square deviation ($M^2$ value) between the point coordinates; 3) the sample point distribution was disrupted, and the $M^2$ value and the significant *P* value were recalculated based on the occurrence probability of the original $M^2$ value in the sampling distribution; 4) the deviation between the corresponding point coordinates was estimated. The smaller the vector residual, the higher the consistency between the two datasets.

The linear discriminant analysis (LDA) effect size (LEfSe), an analytical tool for discovering and interpreting biomarkers in high-dimensional data, was used to identify signature microbiota components and metabolites that were characteristic of the three different age groups. An LDA score > 2 was considered to indicate a significant effect size. The abundances of the signature microbiota components and metabolites were visualized with heat maps and ridgeline plots using the "pheatmap" and "ggridges" functions in R, respectively.

The weighted gene co-expression network analysis (WGCNA) algorithm in the R package (Langfelder and Horvath, 2008) was used to identify genes related to animal phenotypic traits, including age, epithelium morphology, and VFA concentration, with the following settings: sftpower = 14; minModuleSize = 100; and mergeCutHeight = 0.25. The gene network was visualized using Cytoscape (version 3.7.1, Bethesda, MD, USA). Hub genes in the network were selected using the MCODE plugin in Cytoscape (version 2.0) with programmed parameters (degree cutoff: 2; K-Core: 2; and max depth: 100).

Analysis of metabolite traceability and enrichment was performed using MetOrigin (Yu et al., 2022). On the MetOrigin online server, we selected the Simple MetOrigin Analysis (SMOA) mode, which requires a list of metabolites with KEGG or HMDB IDs. SMOA identifies the origins of metabolites based on seven well-known metabolite databases. After loading the dataset, MPEA analysis was carried out, and a bar plot was produced that summarized the total number of metabolites produced by the host, by the microbiota, by co-metabolism, and others.

Spearman's analysis was performed to calculate the correlations between signature microbiota components, rumen phenotypes, critical genes, and metabolites using the "psych" package in R, and the four-level vertical regulatory network was visualized using Cytoscape. Only significant connections ($P < 0.05$, $|r| > 0.5$) were shown in the network.

## 3. Results

### 3.1. Temporal dynamics of rumen microbiota

Regarding alpha diversity, there was no significant difference in microbial richness (Chao1 index) or diversity (Shannon index) across the three ages (Fig. 1A). Regarding beta diversity, distinct clusters among ages were observed ($P < 0.05$). A temporal transition in the microbial community was found on the principal coordinate analysis (PCoA) plot based on Bray–Curtis distance, as the ANOSIM R-value was bigger between goats at 30 d of age (D30) and goats at 90 d of age (D90) ($P < 0.05$) (Fig. 1B; Table S2).

At the phylum level, Bacteroidetes, Firmicutes, and Proteobacteria were the predominant phyla across all ages (Fig. S1A). At the genus level, the rumen microbiota composition showed marked changes with age. For instance, the dominant genera on D30 were *Bacteroides* (7.39%), *Escherichia_Shigella* (9.36%), and *Alloprevotella* (6.40%), while the dominant bacteria on D90 were *Prevotella* (44.23%), and *Succinivibrio* (24.73%) (Fig. S1B).

LEfSe analysis was performed to identify age-associated changes in the rumen microbiota at the genus level, and heatmaps were generated to visualize the dynamic changes in these age-associated bacteria across the three different ages ($P < 0.05$) (Fig. 1C). On d 30, the *Escherichia_Shigella*, *Actinobacillus*, *Actinomyces,* and *Alloprevotella* genera were most abundant. During weaning of goats at 60 d of age (D60), *Ruminococcus*, *Fibrobacter*, *Butyrivibrio,* and *Blautia* were enriched. After weaning (D90), *Prevotella*, *Dialister*, *Megasphaera*, *Olsenella*, *Roseburia*, *Acidaminococcus*, *Sharpea,* and *Oscillibacter* were identified as signature bacteria, and their abundances increased with age.

### 3.2. The growth performance, rumen environment and epithelial development associated with age

As expected, goat kid growth performance indicators, including body weight (BW), starter feed dry matter intake (DMI), and average daily gain (ADG) ($P < 0.05$), differed significantly with age (Table S3). With increasing age, the total VFA concentration increased significantly ($P < 0.001$) (Table 1). The concentrations of acetate, propionate, butyrate, and isovalerate were significantly higher on D90 than on D30 and D60 ($P < 0.001$). In addition, the rumen epithelium developed significantly from D30 to D90 (Fig. 2A). The length and width of the epithelial papillae, muscle thickness, and epithelial thickness were increased significantly on D90, after the introduction of solid feed (D30) and weaning (D60) ($P < 0.05$) (Fig. 2B).

Next, we calculated Spearman correlations among rumen microbiota, rumen fermentation parameters, and epithelial morphology (Fig. 2C). The D30 signature microbiota components, such as *Escherichia_Shigella*, *Actinobacillus,* and *Actinomyces*, were negatively correlated with rumen fermentation parameters and epithelial morphology, while the enriched genera on D90 (i.e.,

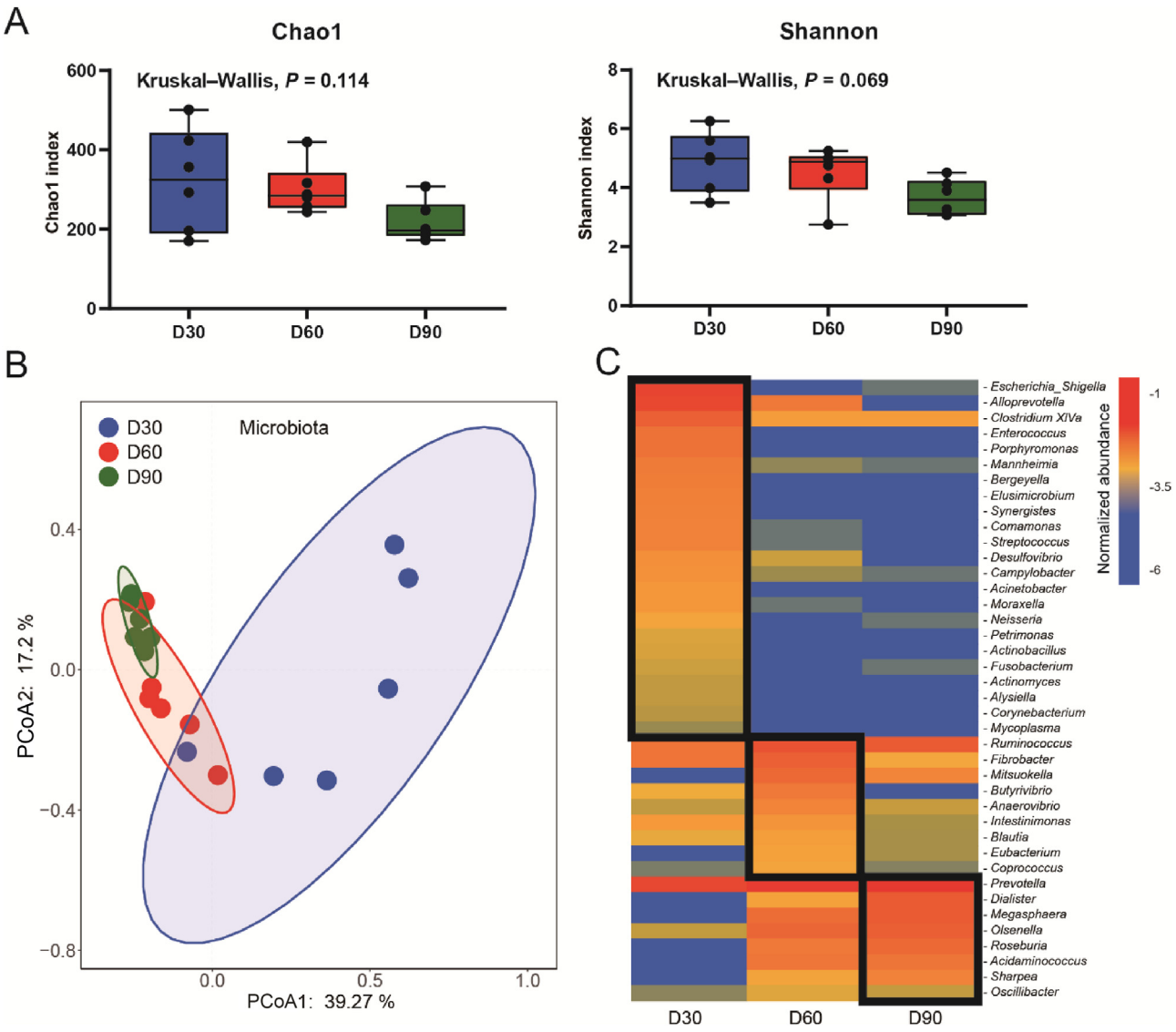


**Fig. 1.** Changes in rumen microbiota with age. (A) The changes in Chao1 and Shannon indexes of rumen microbiota with age. (B) PCoA based on Bray–Curtis distance between rumen microbiota at d 30, 60 and 90. (C) Heatmap depicting the age-associated genera identified by LEfSe algorithm. The abundance of microbiota from high to low is indicated by red to blue in the heatmap. PCoA = principal coordinates analysis; LEfSe = linear discriminant analysis effect size; D30 = goats at 30 d of age; D60 = goats at 60 d of age; D90 = goats at 90 d of age.

**Table 1**
The concentrations of VFA of goat kids at different ages (mmol/L).

| Item | Groups[1] | | | SEM | *P*-value |
|---|---|---|---|---|---|
| | D30 | D60 | D90 | | |
| Total VFA | 20.45$^{b}$ | 43.38$^{b}$ | 113.75$^{a}$ | 11.580 | <0.001 |
| Acetate | 13.73$^{b}$ | 28.55$^{b}$ | 61.70$^{a}$ | 6.100 | <0.001 |
| Propionate | 3.84$^{b}$ | 7.31$^{b}$ | 35.74$^{a}$ | 4.128 | <0.001 |
| Butyrate | 2.29$^{b}$ | 5.74$^{b}$ | 13.73$^{a}$ | 1.427 | <0.001 |
| Isobutyrate | 0.28 | 0.66 | 0.73 | 0.090 | 0.108 |
| Isovalerate | 0.30$^{b}$ | 1.12$^{ab}$ | 1.86$^{a}$ | 0.221 | <0.001 |

VFA = volatile fatty acid.
$^{a,b}$ Values in a row with no common superscripts differ significantly ($P < 0.05$).
[1] D30 = goats at 30 d of age; D60 = goats at 60 d of age; D90 = goats at 90 d of age.

*Prevotella*, *Dialister*, *Olsenella*, *Roseburia*, *Acidaminococcus*, *Megasphaera*, and *Sharpea*) were positively correlated with both rumen fermentation parameters and epithelial morphology ($P < 0.05$).

### 3.3. Rumen epithelial transcriptome changes with age

Transcriptomic analysis was performed to determine changes in gene expression in the rumen epithelium with age. A total of 88.48 Gb of clean data were generated, with an average of 4.92 Gb per sample. The structure of the rumen epithelial transcriptome showed significant clusters at different ages (Fig. S2). Significantly DEGs were also found among the three ages ($P < 0.05$). Compared with D30, there were 2590 DEGs (710 up-regulated genes and 1880 down-regulated genes) on D60 (Fig. 3A) and 2820 DEGs (601 up-regulated genes and 2219 down-regulated genes) on D90 (Fig. 3B). Compared with D60, there were 766 DEGs (375 up-regulated genes and 391 down-regulated genes) on D90 (Fig. 3C). These DEGs were related to "protein binding", "plasma membrane", "integral component of plasma membrane", "inflammatory response", and "collagen-containing extracellular matrix" based on GO analysis (Table S4; Table S5; Table S6).

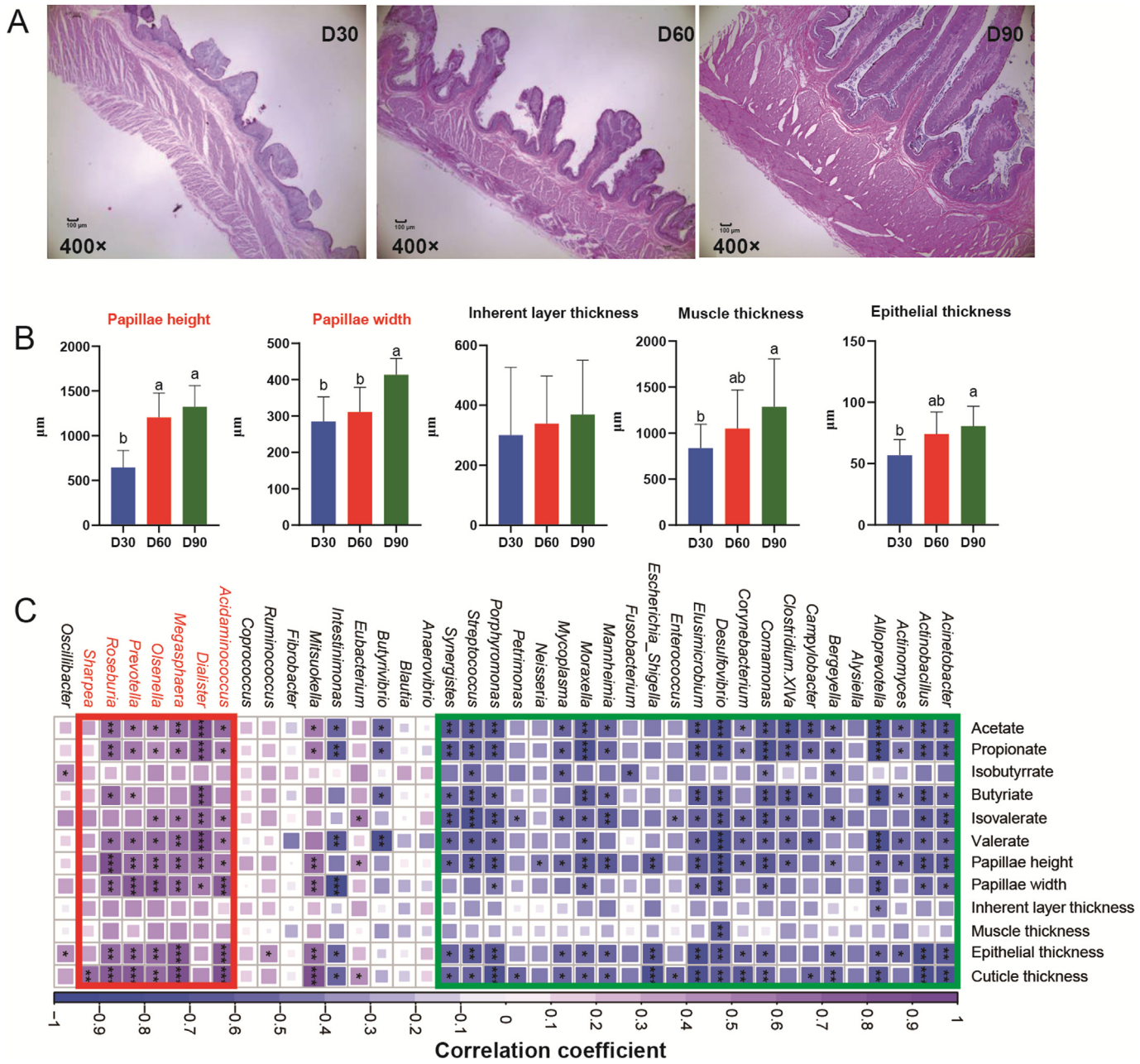


**Fig. 2.** Rumen phenotypes and their relationship with the signature genera. (A) Rumen development regularity of rumen epithelial morphology of goat kids at different ages. The images are displayed via a light micrograph with objective lens (magnification 400×, scale bar = 100 μm). (B) The parameters of rumen epithelium of goat kids at different ages. (C) The Spearman correlations between signature genus and rumen phenotype. Only the significant correlations were marked (*$P < 0.05$, **$0.01 < P < 0.05$, ***$P < 0.01$). D30 = goats at 30 d of age; D60 = goats at 60 d of age; D90 = goats at 90 d of age.

Next, WGCNA was performed to identify correlations among the high-dimensional host transcriptome dataset and animal phenotypes (i.e., rumen fermentation parameters and epithelial morphology). A total of 18,062 host genes were assigned to 12 modules (numbered ME1–ME12). We found that host genes in the ME2 module (261 genes; 1.44% of total genes) correlated positively with most of the goats' phenotypic traits ($P < 0.05$) (Fig. 3D). Using the MCODE plugin in Cytoscape, the hub genes (i.e., *HMGCL*, enoyl-CoA hydratase, short chain 1 (*ECHS1*), propionyl-CoA carboxylase subunit alpha [*PCCA*], and hydroxyacyl-CoA dehydrogenase [*HADH*]) in the ME2 module were identified as core nodes connecting other genes (Fig. 3E). In addition, KEGG enrichment analysis showed that the genes in the ME2 module were mainly enriched in the "butanoate metabolism", "propanoate metabolism", "synthesis and degradation of ketone bodies", and "valine, leucine and isoleucine degradation" metabolic pathways (shown in red) and in signaling pathways (shown in blue) such as "peroxisome", "oxidative phosphorylation", "protein kinase AMP-activated catalytic subunit alpha 1 (AMPK) signaling pathway" and "PPAR and mTOR signaling pathway" ($P < 0.05$) (Fig. 4A). Visualization of associations between the hub genes and important KEGG-predicted pathways (Fig. 4B) showed that *HMGCS2* was associated with "synthesis and degradation of ketone bodies", "butanoate metabolism", and the "PPAR and mTOR signaling pathway". *BDH1* was associated with "synthesis and degradation of ketone bodies" and "butanoate metabolism". *ECHS1* was linked with "butanoate

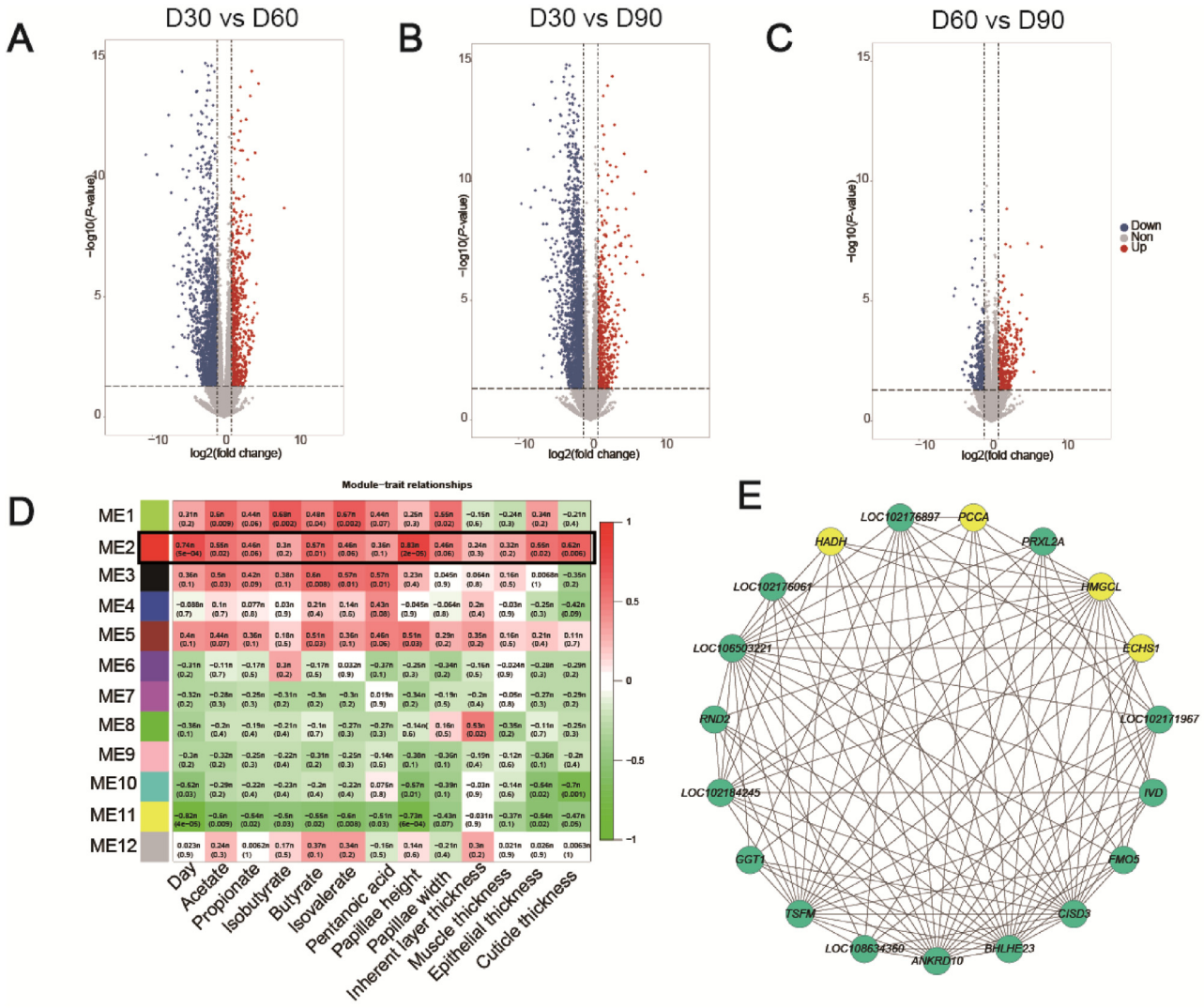


**Fig. 3.** The identification and analysis of phenotype-related genes in host transcriptome. The volcano plot of differentially expressed genes in pair-wise comparisons of D30 vs. D60 (A), D30 vs. D90 (B) and D60 vs. D90 (C). The red dots represent the up-regulated genes, the blue dots represent the down-regulated genes, and the grey dots represent unchanged genes. (D) The association between weighted gene co-expression network analysis (WGCNA) modules of the host transcriptome and animal phenotype. (E) The core network of hub genes in ME2 module. *HADH* = hydroxyacyl-CoA dehydrogenase; *PCCA* = propionyl-CoA carboxylase subunit alpha; *PRXL2A* = anti-PRXL2A rabbit polyclonal antibody; *HMGCL* = 3-hydroxy-3-methylglutaryl-CoA lyase; *RND2* = Rho family GTPase 2; *ECHS1* = Enoyl-CoA hydratase, short chain 1; *GGT1* = gamma-glutamyltransferase 1; *IVD* = isovaleryl-CoA dehydrogenase; *TSFM* = Ts translation elongation factor, mitochondrial; *FMO5* = flavin containing dimethylaniline monoxygenase 5; *ANKRD10* = ankyrin repeat domain 10; *CISD3* = CDGSH iron sulfur domain 3; *BHLHE23* = basic helix-loop-helix family member e23. ME = module; D30 = goats at 30 d of age; D60 = goats at 60 of age; D90 = goats at 90 d of age.

metabolism", "fatty acid metabolism" and "Propanoate metabolism". *PPARG* was correlated with the "PPAR and AMPK signaling pathway". The adenosine triphosphate (ATP) synthase peripheral stalk subunit F6 (*ATP5PF*) gene was linked with "metabolic pathways" and "oxidative phosphorylation". The ring finger protein 152 (*RNF152*) and Ras-related GTP binding D (*RRAGD*) genes were associated with the "mTOR signaling pathway".

Based on the results of the microbiota, VFA production, epithelial transcriptomics, and morphology analyses, we briefly summarized the possible biological mechanism by which the microbiota regulates rumen epithelial development (Fig. S3). With increasing age, the rumen microbiota, including *Prevotella*, *Dialister, Roseburia*, *Megasphaera,* and *Sharpea*, increase in abundance and produce more VFA (i.e., acetate, propionate, and butyrate), which could regulate signaling or metabolic pathways, such as the "PPAR and mTOR signaling pathway," "propanoate metabolism" pathway, and "butanoate metabolism" pathways, through up- or down-regulation of major genes (i.e., *HMGCS2*, *PPARG*, *ECHS1*, *RNF152*). For instance, butyrate could stimulate expression of *PPARG* and *HMGCS2*, which encode components of the PPAR signaling pathway. This could then activate the "synthesis and degradation of ketone bodies" and "butanoate metabolism" pathways. At the same time, genes associated with the "oxidative phosphorylation" signaling pathway are up-regulated to provide energy for the corresponding metabolic pathways. Finally, alterations in these pathways can cause significant modulations in rumen development, such as increased papilla length and width and improved epithelial and muscle thickness, as observed in this study. We next analyzed the metabolomics of the rumen epithelial tissue from D30, D60, and D90 to validate these predicted biological processes.

### 3.4. Rumen epithelial metabolomics are influenced by age

A total of 657 metabolites were detected in the rumen epithelium using non-targeted LC-MS based metabolomics. The composition and structure of the metabolome showed distinct differences

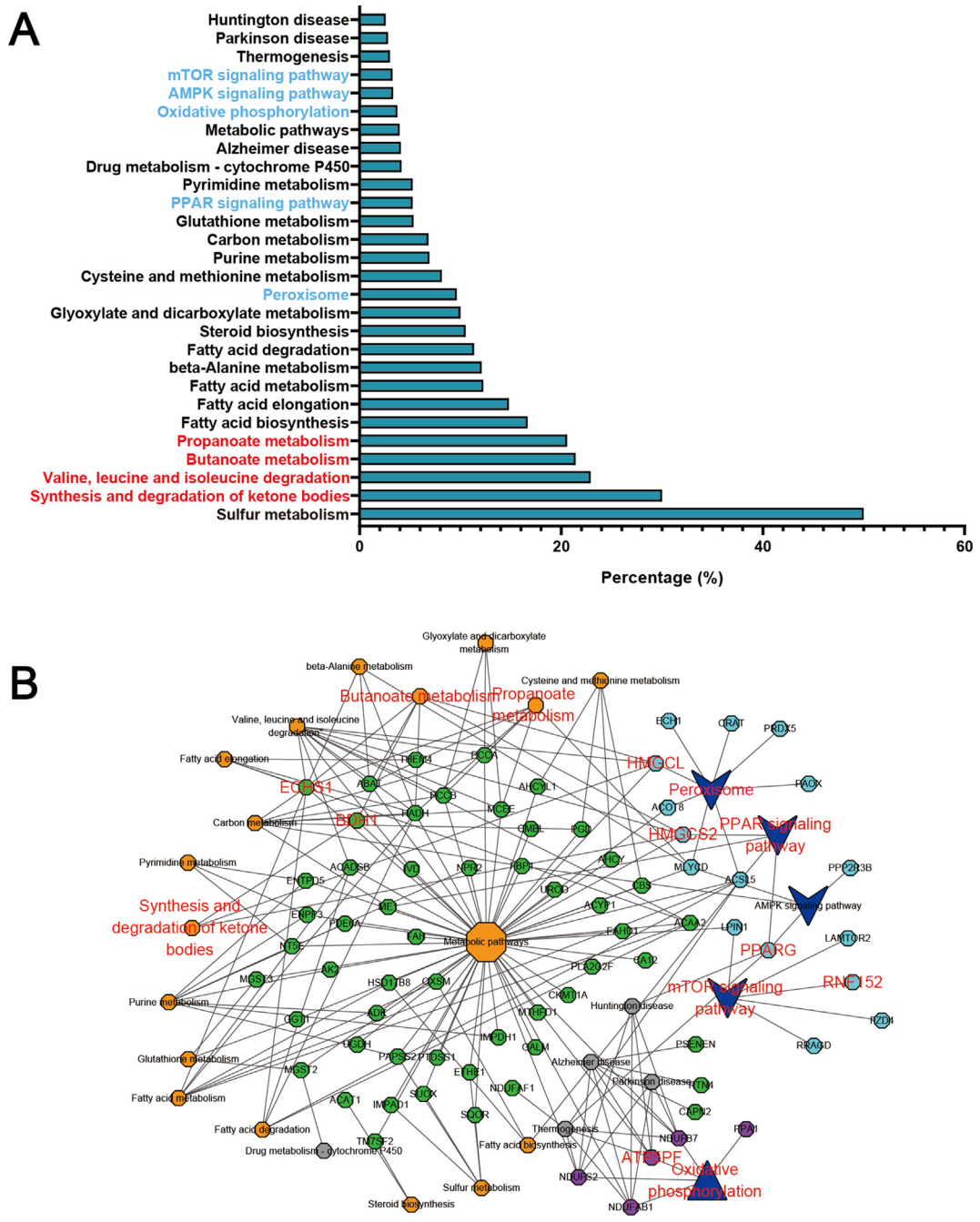


**Fig. 4.** The function analysis of genes in WGCNA ME2. (A) KEGG pathway enrichment analysis for the ME2 module genes. The significant pathways related to nutrition metabolism are marked in red, and the pathways related to signal transduction are marked in blue. (B) The association network of KEGG pathways and related genes. The nodes of the metabolic pathway are in orange, and its related genes are in green. The nodes of signaling pathways are in deep blue, and its related genes are in light blue. The critical pathway and gene name are marked in red. WGCNA = the association between weighted gene co-expression network analysis; ME = module; KEGG = Kyoto Encyclopedia of Genes and Genomes.

among D30, D60, and D90 (Fig. 5A, Table S7). Using LEfSe analysis, we identified a total of 309 differentially abundant metabolites across the three ages ($P < 0.05$) (Fig. 5B). Some metabolites, including D-Galactose, Glucose 6-phosphate and alpha-D-Glucose, were enriched on D30 and decreased in abundance with age. Next, we classified the age-associated metabolites into major biological molecule types (Fig. 5C). We found that the concentration of amino acid metabolites increased gradually with age (D30: 19.19%; D60: 23.96%; D90: 25.66%), while metabolites associated with carbohydrates showed the opposite pattern (D30: 16.16%; D60: 8.33%; D90: 7.08%).

Next, MetOrigin analysis was performed to determine the sources of epithelial metabolites; that is, whether they were produced by the host, bacteria, or both. We found that 101 of the 657 detected metabolites were produced by the microbiota, 240 by the host, and 220 by both the host and the microbiota (Fig. S4). To better characterize the important metabolites related to age, LEfSe outputs were also determined using MetOrigin analysis (Fig. S5). A total of 58 metabolites, including homoisocitrate, D-arabinose, and indican, were annotated as having a microbiota origin. In contrast, the host-related metabolites included 114 age-related metabolites, such as D-galactose, glucose 6-phosphate, alpha-D-glucose, (R)-3-

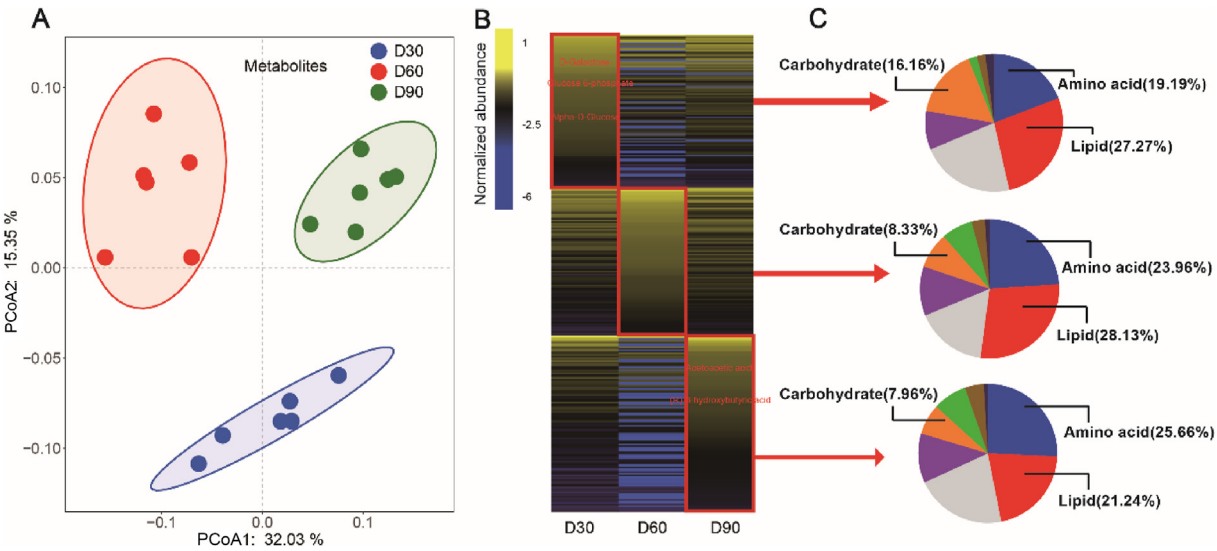


**Fig. 5.** The changes in rumen epithelial metabolism with age. (A) PCoA of Bray–Curtis distances between rumen epithelial metabolism profile at different ages. (B) The identification of age-related metabolites using LEfSe. The abundance of metabolites from high to low is indicated by yellow to blue in the heatmap. (C) The composition of age-related metabolites at higher classification level. PCoA = principal-coordinate analysis; LEfSe = linear discriminant analysis effect size; D30 = goats at 30 d of age; D60 = goats at 60 d of age; D90 = goats at 90 d of age.

hydroxybutyric acid (BHBA), acetoacetic acid (ACAC), and capric acid.

KEGG enrichment analysis of host metabolites were performed. On D30, before weaning, "galactose metabolism" was the most abundant metabolic pathway, as demonstrated by enrichment in the following metabolites: D-galactose, glucose 6-phosphate, alpha-D-glucose, D-glucose, D-glucuronic acid, and glucuronic acid (Fig. 6A and B). On D60, amino acid metabolic pathways were identified as the signature metabolic pathways, such as the "glutathione metabolism," "valine, leucine and isoleucine biosynthesis," and "arginine biosynthesis" pathways, owing to the higher abundances of L-glutamic acid, L-cysteine, L-lactic acid, and fumaric acid (Fig. 6C and D). However, on D90, the pathways related to "butanoate metabolism" and "synthesis and degradation of ketone bodies" were dominant, with increased abundance of metabolites such as BHBA, ACAC, and pyruvic acid (Fig. 7E and F). In addition, these age-related metabolites were the hub nodes associated with metabolic pathways and other metabolites (Fig. 6B–D, F).

### 3.5. Associations among the rumen microbiota, the epithelial transcriptome, and the metabolome

To identify novel associations among the rumen microbiota, the epithelial transcriptome, and the metabolome, we performed MCIA (Meng et al., 2014) which can assess relationships and trends in multiple high-dimensional datasets by projecting them to the same dimensionality (Fig. S6). The different datasets (rumen content microbiota, host transcriptome, and metabolome) from each animal were visualized as being connected by lines, with the length of the lines representing the degree of difference between the datasets. All three datasets showed good consistency on D30, D60, and D90. There were clear distances between datasets from different timepoints that increased with age (Fig. S6A). In addition, the pseudo-eigenvalues that were correlated with the first two PCs of each dataset were calculated to describe the contribution of each dataset to the total variance and correlation between different datasets. The host transcriptomics explained the massive variation in both axis 1 and axis 2, and the rumen microbiota explained the largest variation in axis 1 (Fig. S6B). There may be a stronger correlation between the rumen microbiota and the host transcriptome than between the rumen microbiota and the epithelial metabolome, as indicated by their close distance at axis 1.

In addition, using Procrustes analysis, we found that the epithelial transcriptome was correlated significantly with the rumen microbiota ($M^2 = 2.0858$, $P = 0.011$, Fig. S7A) and the epithelial metabolome ($M^2 = 1.1859$, $P = 0.007$) (Fig. S7B) regardless of age, while there was no significant association between the rumen microbiota and the epithelial metabolome, consistent with the MCIA results (Fig. S7C).

### 3.6. Diet shapes age-specific host metabolomics in young ruminants

Permutational multivariate analysis of variance (PERMANOVA) was performed to identify the mechanism underlying the assembly of the rumen microbiota, the epithelial transcriptome, and the metabolome. Factors including age, diet, VFA production, and epithelial morphology, were examined (Table 2). We first performed PERMANOVA using univariate models. Age was the significant factor influencing the rumen microbiota and the epithelial transcriptome, with 18.24% and 21.11% variation, respectively, followed by diet, with 8.09% and 16.25% variation, respectively ($P < 0.05$) (Table 2(a)). However, for epithelial metabolomics, diet was the most important factor in the multivariate model, with 27.76% variation, while age explained 15.78% of the variation ($P < 0.05$).

In another PERMANOVA model constructed to determine which nutrients in the diet contributed most to rumen development, -consumption had the strongest effect on shaping the rumen microbiota, the epithelial transcriptome, and the metabolome, followed by ADF intake. Specifically, NDF from a solid diet was the major factor driving rumen development ($P < 0.05$) (Table 2(b)).

Next, we evaluated the impact of VFA and epithelial morphological parameters on the rumen microbiota, the epithelial transcriptome, and the metabolome and found that butyrate and papillae height had significant effects on these three high-dimensional datasets were. Moreover, propionate had significant effects on the rumen microbiota and the epithelial metabolome,

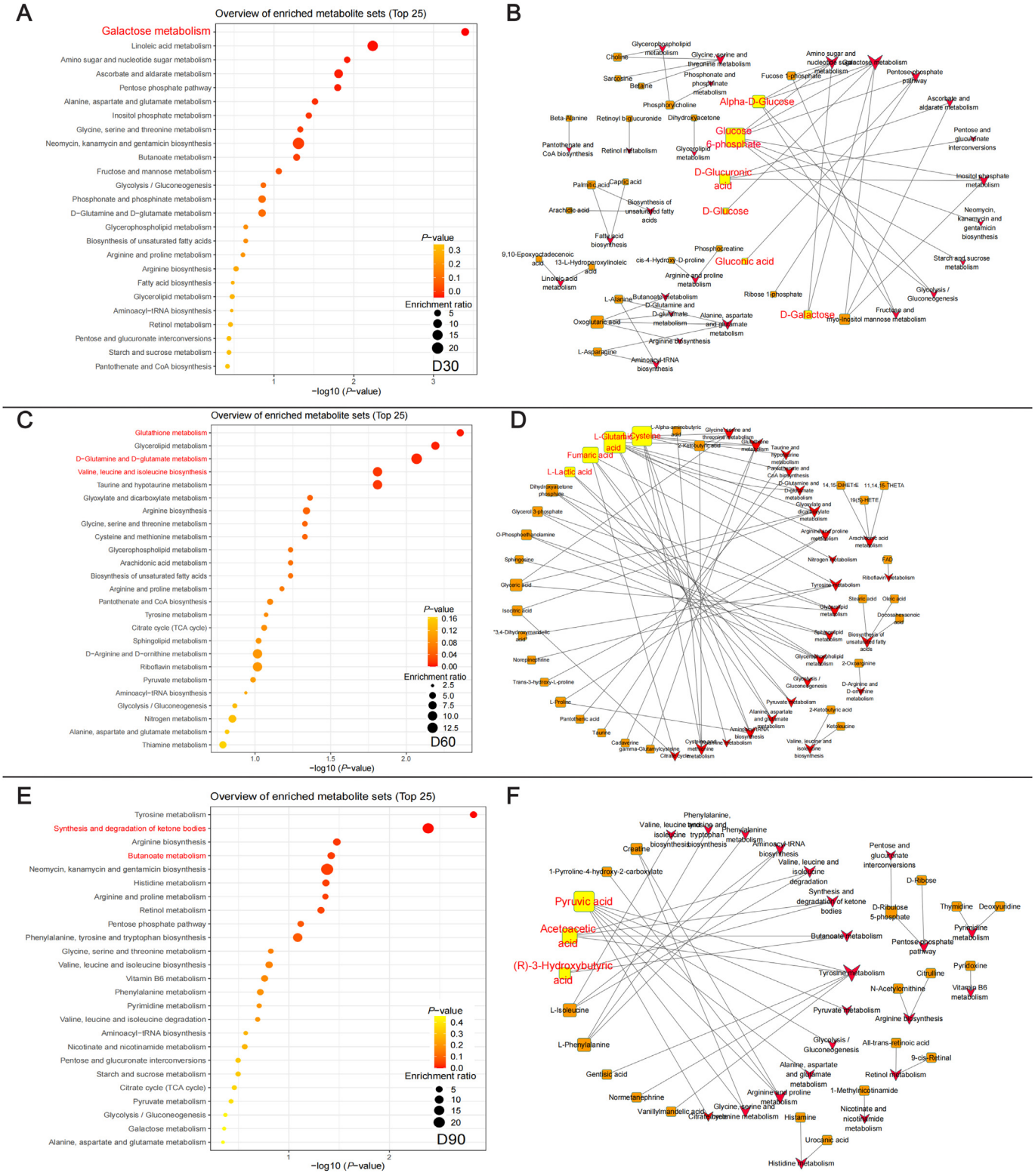


**Fig. 6.** The functional analysis of age-related metabolites derived from host. (A-B) KEGG pathway enrichment analysis of metabolites and its association network on D30 (C-D) KEGG pathway enrichment analysis of metabolites and its association network on D60. (E-F) KEGG pathway enrichment analysis of metabolites and its association network on D90. The major metabolic pathways are marked in red on the bubble chart and the nodes of signature metabolites are marked in light yellow in the association network. The critical metabolites are marked in red. KEGG= Kyoto Encyclopedia of Genes and Genomes; D30 = goats at 30 d of age; D60 = goats at 60 d of age; D90 = goats at 90 d of age.

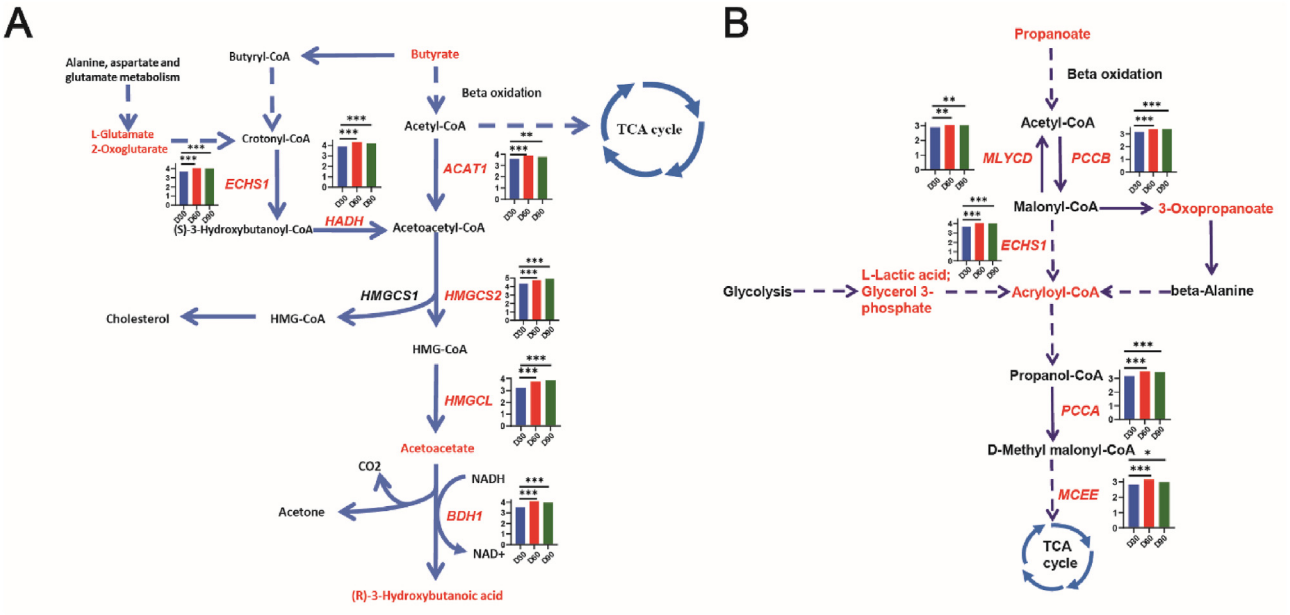


**Fig. 7.** The identification of signature metabolic pathways combined outputs from rumen epithelial transcriptome and metabolomics. (A) Butanoate metabolism (B) Propanoate metabolism. The genes and metabolites in red represent their active expression with age. The histogram indicates the expression levels of these genes at different ages. (*$P < 0.05$, **$0.01 < P < 0.05$, ***$P < 0.01$). *ECHS1* = enoyl-CoA hydratase, short chain 1; *ACAT1* = acetyl-CoA acetyltransferase 1; *HADH* = hydroxyacyl-CoA dehydrogenase; *HMGCS1* = 3-hydroxy-3-methylglutaryl-CoA synthase 1; *HMGCS2* = 3-hydroxy-3-methylglutaryl-CoA synthase 2; *HMGCL* = 3-hydroxy-3-methylglutaryl-CoA lyase; *NADH* = nicotinamide adenine dinucleotide; *MLYCD* = malonyl-CoA decarboxylase; *PCCB* = propionyl-CoA carboxylase subunit beta; *PCCA* = propionyl-CoA carboxylase subunit alpha; *MCEE* = methylmalonyl-CoA epimerase. D30 = goats at 30 d of age; D60 = goats at 60 d of age; D90 = goats at 90 d of age.

**Table 2**
PERMANOVA analysis of the factors affecting the rumen microbiota, epithelial transcriptome, and epithelial metabolomics (multivariate models)[1].

| Rumen microbiota | $R^2$ | *P*-value | Host transcriptome | $R^2$ | *P*-value | Host metabolomic | $R^2$ | *P*-value |
|---|---|---|---|---|---|---|---|---|
| (a) | | | | | | | | |
| Age | 18.24 | 0.001 | Age | 21.11 | 0.001 | Age | 15.78 | 0.002 |
| Diet | 8.09 | 0.069 | Diet | 16.25 | 0.005 | Diet | 27.76 | 0.001 |
| (b) | | | | | | | | |
| NDF intake | 18.27 | 0.001 | NDF intake | 21.54 | 0.002 | NDF intake | 29.50 | 0.001 |
| ADF intake | 8.02 | 0.066 | ADF intake | 15.62 | 0.005 | ADF intake | 13.94 | 0.002 |
| (c) | | | | | | | | |
| Butyrate | 11.99 | 0.006 | Butyrate | 14.8 | 0.043 | Butyrate | 13.30 | 0.014 |
| Propionate | 10.92 | 0.003 | Propionate | 2.36 | 0.828 | Propionate | 13.69 | 0.011 |
| Acetate | 4.75 | 0.511 | Acetate | 3.09 | 0.712 | Acetate | 5.64 | 0.219 |
| Papillae height | 8.11 | 0.040 | Papillae height | 17.14 | 0.026 | Papillae height | 11.29 | 0.023 |
| Papillae width | 3.59 | 0.831 | Papillae width | 2.24 | 0.876 | Papillae width | 4.90 | 0.344 |
| Muscle thickness | 5.84 | 0.258 | Muscle thickness | 1.93 | 0.907 | Muscle thickness | 4.63 | 0.419 |
| Epithelial thickness | 8.00 | 0.048 | Epithelial thickness | 12.75 | 0.085 | Epithelial thickness | 3.28 | 0.700 |

PERMANOVA = permutational multivariate analysis of variance; NDF = neutral detergent fiber; ADF = acid detergent fiber.
[1] PERMANOVA analysis was performed with three sequential orders listed in the Table: (a) age + diet; (b) NDF intake + ADF intake; (c) butyrate + propionate + acetate + papillae height + papillae width + muscle thickness + epithelial thickness + cuticle thickness.

explaining about 11% and 14% of the variation, respectively ($P < 0.05$) (Table 2(c)).

### 3.7. The rumen microbiota and its metabolites (VFA) improve epithelial gene transcription and metabolism

We further assessed how rumen VFA influence gene expression and the abundance of related metabolites by mapping the major 'butanoate metabolism' and 'propanoate metabolism' KEGG pathways that were identified as being activated with age by both epithelial transcriptomics and metabolomics (Fig. 7). In the 'butanoate metabolism' pathway, the expression of six genes (*ACAT1*, *HMGCS2*, *HMGCL*, *BDH1*, *ECHS1*, and *HADH*) related to the ketone synthesis sub-pathway and the abundance of four metabolites (L-glutamate, 2-oxoglutarate, and the ketone bodies acetoacetate and (R)-3-hydroxybutanoic acid) were increased significantly on D60 and D90 compared with D30, resulting in increased conversion of *NADH* to $NAD^+$, which provides energy for epithelial growth ($P < 0.05$) (Fig. 8A). In the 'propanoate metabolism' pathway, the expression levels of five genes (*ECHS1*, malonyl-CoA decarboxylase (*MLYCD*), propionyl-CoA carboxylase subunit beta [*PCCB*], *PCCA*, and *MCEE*) and the abundance of four metabolites (L-lactic acid, glycerol 3-phosphate, acryloyl-CoA, and 3-oxopropanoate) were also increased significantly on D60 and D90 compared with D30 (Fig. 8B).

Finally, the complex interactions among the rumen microbiota, VFA, the epithelial transcriptome, and the metabolome within a four-level vertical regulatory network were assessed using the Spearman algorithm (Fig. 8). Rumen microbiota components, including *Prevotella*, *Dialister*, and *Roseburia*, that increased in

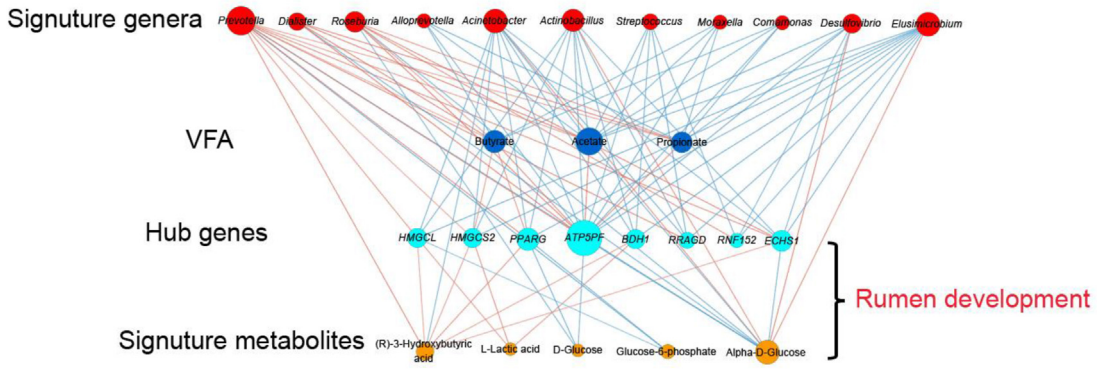


**Fig. 8.** Network analysis of the interaction among rumen microbiota, rumen phenotypes, epithelial transcriptome and metabolomics. Nodes in red represent the signature genera at different ages. Nodes in dark blue represent the animal phenotypes. Nodes in light blue represent critical genes related to rumen epithelial development. Nodes in orange represent the signature metabolites at different ages. The size of nodes represents the degree of connection, and the color of the line represents the positive (red) or negative correlation (blue). VFA = volatile fatty acid; *HMGCL* = 3-hydroxy-3-methylglutaryl-CoA lyase; *HMGCS2* = 3-hydroxy-3-methylglutaryl-CoA synthase 2; *PPARG* = peroxisome proliferator activated receptor gamma; *ATP5PF* = ATP synthase peripheral stalk subunit F6; *BDH1* = 3-hydroxybutyrate dehydrogenase 1; *RRAGD* = Ras related GTP binding D; *RNF152* = ring finger protein 152; *ECHS1* = enoyl-CoA hydratase, short chain 1.

abundance with age showed the most positive correlations with VFA (butyrate, acetate, propionate) ($P < 0.05$). Butyrate served as a hub node connecting age-related signature microbiota and critical epithelial genes at level 2. At level 3, *HMGCS2*, *PPARG*, and *ECHS1* served as a bridge linking VFA and epithelial metabolites ((R)-3-hydroxybutanoic acid, L-lactic acid, etc.). The hub genes and metabolites at levels 3 and 4 were strongly associated with rumen development ($P < 0.05$). Altogether, these findings suggest that VFA derived from the rumen microbiota could influence the expression of rumen epithelium genes, thereby impacting epithelial metabolism and resulting in improved growth of the rumen epithelium.

## 4. Discussion

Although our understanding of the rumen microbiome and tissue development during early life is increasing (Chai et al., 2021; Malmuthuge et al., 2019), the interactions between the microbes and host at different ages remain unclear. In this study, we integrated analyses of the rumen microbiota, the epithelial transcriptome, and the metabolome from preweaning to postweaning in goats to explore interactions between the ruminal microbiota and the host. Our results confirmed that the abundance of rumen microbiota–derived VFA (butyrate, acetate, propionate) increased with age and solid diet intake, resulting in "increased activation of the "propanoate metabolism" and "butanoate metabolism" pathways via up-regulation of gene expression and metabolites in the rumen epithelium, which subsequently promoted rumen development. Moreover, to our knowledge, this is the first study to validate the temporal association between rumen microbes and the host transcriptome by performing epithelial metabolomics analysis. Our findings suggest that microbiota-derived VFA regulate host gene expression and metabolism.

Changes in the structure and diversity of the rumen microbiota with age have been reported previously (Jiao et al., 2024; Yin et al., 2021) and were also found in our study. Dynamic adjustment of dietary intake is likely the main reason for these changes, as the goats' diet changed from milk plus starter to only starter from pre- to postweaning (Abdelsattar et al., 2022; Meale et al., 2016). Correspondingly, the abundance of some bacteria changed (Mizrahi et al., 2021; Moraïs and Mizrahi, 2019). For instance, the genera *Actinobacillus* and *Petrimonas* decreased in abundance with age. *Actinobacillus* can ferment succinic acid from monosaccharides such as glucose and galactose, which provide the substrate for the tricarboxylic acid cycle (Chang et al., 2015; Karama et al., 2020). *Petrimonas* can ferment sugars and amino acids to acetate and propionic acid (Maus et al., 2020). The abundance of certain microbes, including *Blautia*, *Butyrivibrio*, *Fibrobacter*, and *Ruminococcus*, which produce VFA via degradation of dietary fiber (Liu et al., 2021; Paillard et al., 2007), was specifically enriched on D60. Other microbes, such as *Prevotella*, *Megasphaera*, *Roseburia,* and *Sharpea*, increased in abundance with age and were positively correlated with VFA concentrations. *Prevotella* is an efficient user of fiber and non-fiber carbohydrates, and is involved in degrading oligopeptides into amino acids (Li et al., 2020). *Megasphaera* is an important genus in the rumen that metabolizes lactate in animals fed a high-concentrate diet (Chen et al., 2019). *Roseburia* can produce VFA, especially butyrate (Zhao et al., 2022). Changes in dietary components could stimulate the metabolic activity of *Roseburia* (Imhann et al., 2018; Van den Abbeele et al., 2013). *Sharpea* induces acidogenic bacteria to consume lactic acid, which produces acetate and butyrate, and the abundance of this genus increased when the goats were fed with starter (Kamke et al., 2016; Lin et al., 2019). Therefore, from preweaning to postweaning, age and consumption of solid feed shapes the structure and composition of the rumen microbiota.

Transcriptomics has been used previously to study the rumen epithelial tissue (Connor et al., 2013; Lin et al., 2019). In this study, we found that the temporal changes in rumen epithelial gene expression were correlated with age and animal phenotypes. Through KEGG annotation, we found that these hub genes were associated with metabolomic pathways involved in VFA and amino acid production, which is consistent with previous studies (Chai et al., 2021; Li et al., 2012; Lin et al., 2019). Notably, up-regulation of genes related to the oxidative phosphorylation signaling pathway was also observed in this study, implying that VFA might play multiple important roles in epithelial development and metabolism (Beaumont et al., 2020; Coutzac et al., 2020). Therefore, microbiota-derived VFA could regulate the epithelial transcriptome to improve rumen development.

The use of non-targeted metabolomics in this study was intended to enable quick and reliable classification of small molecule biomarkers for age-related characteristics of the rumen epithelium. Many studies have performed microbial metabolomics analyses to identify host–microbe interactions, since microbial metabolites in the gut can enter the host tissues and circulation (Han et al., 2021). In ruminants, metabolomics analysis has only rarely been used to study the rumen. Several studies have focused on rumen microbial metabolomics (Lin et al., 2019; Wang et al., 2023; Xue et al., 2020a), while only one study assessed rumen epithelial metabolomics and found that pyruvate metabolism in the goat epithelium was enriched by high-grain diets compared

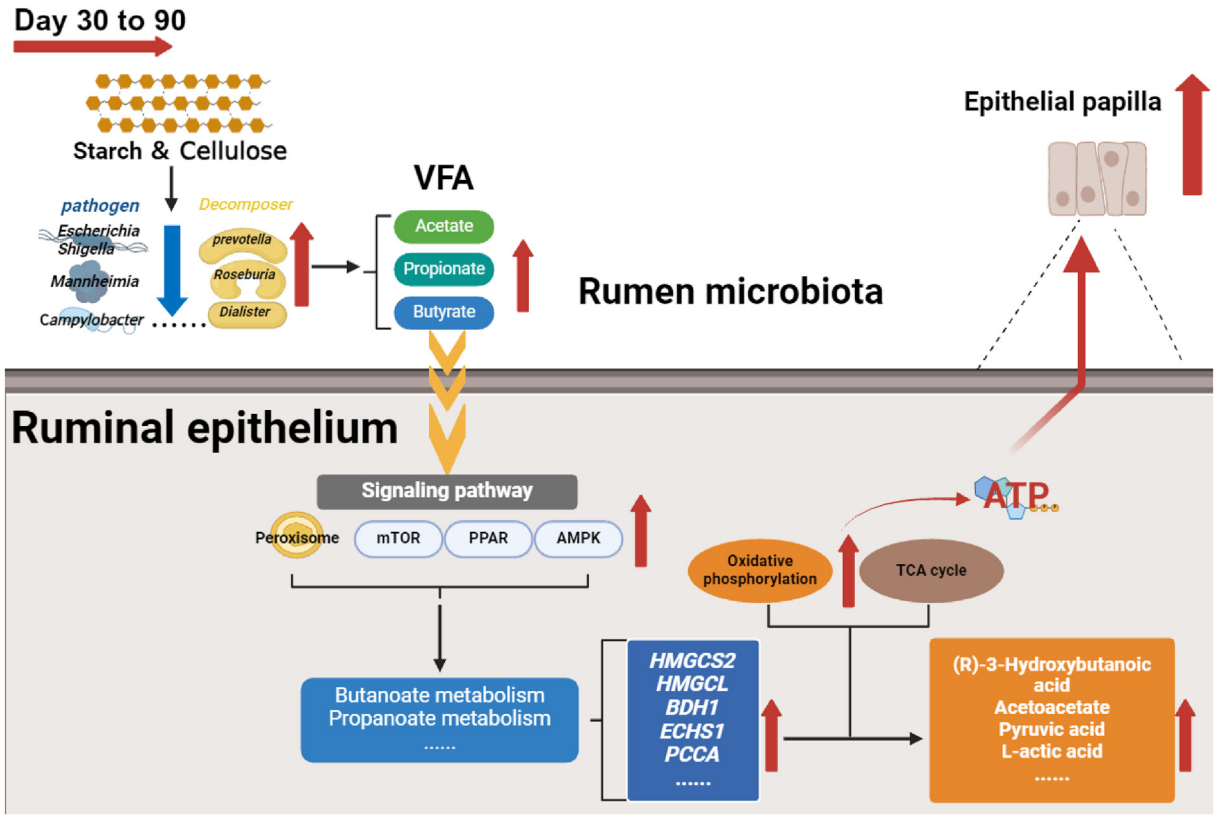


**Fig. 9.** Volatile fatty acids fermented by rumen signature bacteria dominate the rumen epithelium growth and metabolism in early life of goat kids. From day 30 to 90, change of diet from milk to solid diet caused increases in fiber degraders (*Prevotella*, *Roseburia* and *Sharpea*) and VFA concentrations. Accumulation of VFA, especially butyrate, dominated the energy metabolism of rumen epithelium by regulating the mTOR and PPAR signaling pathways, and activated oxidative phosphorylation to produce energy for the growth and proliferation of rumen papillae. VFA = volatile fatty acid; *mTOR* = mammalian target of rapamycin; *PPAR* = peroxisome proliferator activated receptor; *AMPK* = adenosine 5'-monophosphate (AMP)-activated protein kinase; *HMGCS2* = 3-hydroxy-3-methylglutaryl-CoA synthase 2; *HMGCL* = 3-hydroxy-3-methylglutaryl-CoA lyase; *BDH1* = 3-hydroxybutyrate dehydrogenase 1; *ECHS1* = enoyl-CoA hydratase, short chain 1; *PCCA* = propionyl-CoA carboxylase subunit alpha; *TCA* = tricarboxylic acid cycle; ATP = adenosine triphosphate.

with a hay diet (Guo et al., 2019). Consistent with our transcriptomics data, we also observed changed in epithelial metabolomics from preweaning to postweaning. The signature metabolites for D30 were alpha-D-Glucose, Glucose 6-phosphate, D-Glucose, and D-Galactose, which were enriched in the galactose metabolism pathway. As breast milk is the only nutrient source before D30, it is not surprising that these lactose secondary products accumulated in the rumen epithelium. During weaning, rumen epithelial metabolites were enriched with more active amino acids, including L-glutamic acid, L-cysteine, and L-lactic acid, which are associated with the glutathione metabolism, valine, leucine, and isoleucine biosynthesis, and arginine biosynthesis metabolic pathways. This may be due to cellular growth and biosynthesis in the rapidly developing rumen. Furthermore, on D90 after weaning, BHBA and ACAC abundances were increased in the rumen epithelium. The mature epithelium can provide two-thirds of the energy that the host needs by converting butyrate to BHBA (in a process known as ketogenesis) (Xue et al., 2020b). As products of ketogenesis, BHBA and ACAC are considered important hallmarks of rumen epithelium development (Wang et al., 2016). Therefore, corresponding with a dietary change from milk to a solid diet, butyrate-based ketone body metabolism replaced glucose metabolism as the primary form of metabolism in the mature rumen epithelium.

Rumen development is affected by multiple factors such as host genetics, age, diet, weaning, environment, health, disease, and antibiotics (Chai et al., 2024a). Our previous study confirmed that a solid feed, and especially NDF content, is the main factor influencing rumen microbiota structure and the epithelial transcriptome in goat kids on d 60 (Chai et al., 2021). However, the effect of age was not considered. In this study, we found that age was the most important factor influencing the rumen microbiota and the epithelial transcriptome, followed by diet and related products (butyrate and propionate). This is because the rumen experiences dramatic changes from the suckling period during weaning and postweaning. In addition, we found that VFA produced by the rumen microbiota might directly regulate the transcriptome, rather than regulating rumen epithelium metabolism. Volatile fatty acids activate many signaling pathways via a variety of factors, such as histone deacetylase, G-protein–coupled receptors, and acetyl-CoA production (Kim, 2021). Thus, VFA production, which is affected by the microbiota and diet, can regulate rumen epithelial gene expression, resulting in changes in the abundance of epithelial metabolites. Butyrate stimulates changes in rumen epithelial morphology and provides energy, and up-regulation of genes encoding factors that convert butyrate to ketones as an indicator of mature rumen epithelium metabolism (Lane et al., 2000, 2002). We found that *HMGCS2* expression correlated positively with the abundance of butyrate generated by microbiota, which also correlated with BHBA and L-lactic acid levels. In addition, “butanoate metabolism” and “propanoate metabolism” were the pathways that were most often predicted to be activated with age by both transcriptomic and metabolomic analysis. Many of the molecules within these two pathways are ultimately involved in the production of ketone bodies, the construction of lipids, or as precursors to the citrate cycle, glycolysis, or glutamate synthesis.

From the suckling stage to postweaning, rumen ketogenesis increased, as indicated by the increase in the expression of *HMGCS2*, *ACAT1*, *HMGCL*, *BDH1*, and *PPARG*, which encode factors involved in the generation of ketone bodies. Recent studies have reported that BHBA accumulation and increased *HMGCS2* expression, which are associated with ketogenesis, strengthen the ability of gut epithelial cells to proliferate, differentiate, and maintain gut homeostasis (Cheng et al., 2019; Wang et al., 2017). *HMGCS2* expression is mainly promoted by peroxisome proliferator-activated receptor (*PPARs*) (Wang et al., 2018; Zhang et al., 2019) and inhibited by mTOR (Howell and Manning, 2011). Short-chain fatty acids are efficient ligands that can effectively induce *PPARs* to promote transcription of the target gene *HMGCS2* (den Besten et al., 2015; Zhuang et al., 2023b). In contrast, the mTOR pathway, which is critical for regulating growth and proliferation, can be inhibited by increased *RNF152* expression (Okamoto et al., 2020). Hence, butyrate produced by fiber decomposers (e.g., *Prevotella*) mainly promotes ketone metabolism and rumen development through the PPAR and mTOR signaling pathways. Alternatively, butyrate serves as a dominant energy source via β-oxidation and the tricarboxylic acid cycle in mitochondria (Salvi and Cowles, 2021). With increasing age, butyrate production leads to increased expression of *ATP5PF*, *NDUFAB1*, *NDUFB7*, and *NDUFS2*, which encode components of the oxidative phosphorylation pathway. *ATP5PF* encodes the ATP synthase subunit in the mitochondrial membrane (F1F0 ATP synthase or Complex V), which participates in ATP assembly (Wu et al., 2016). The *NDUFAB1*, *NDUFB7*, and *NDUFS2* gene products are responsible for electron transfer from *NADH* to the respiratory chain, which is required for oxidative phosphorylation. *NADH* is derived from biochemical metabolism processes, such as ketogenesis, glycolysis, the tricarboxylic acid cycle, and lipid oxidation (Wilson, 2017). *NADH* accumulation activates oxidative phosphorylation and increases the expression of related genes to meet the higher demand for ATP to enable rumen growth. Expression of *ECHS1*, which encodes a critical enzyme in mitochondrial butyrate β-oxidation metabolism, increases with age. Moreover, metabolomics analysis of the rumen epithelium validated the activation of these signaling pathways. Therefore, our findings suggest that VFA produced by the rumen microbiota stimulate increased expression of epithelial genes and increased production of metabolites associated with ketogenesis, which promotes rumen development.

## 5. Conclusions

In conclusion, we found that age is the major driver of rumen microbiota and rumen epithelial development in goats. Butyrate and propionate produced by signature bacteria activated energy metabolism and rumen epithelium development by regulating the mTOR and PPAR signaling pathways. Moreover, rumen epithelial metabolomics analysis revealed that butyrate-regulated ketogenesis may be critical for rumen development. BHBA and ACAC, which were highly abundant by D90, could be marker metabolites for rumen development (Fig. 9). The interactions observed between the rumen microbiota and the host provide evidence that manipulation of the rumen microbiome is an effective approach to improving rumen development and host growth.

## Credit Author Statement

**Yimin Zhuang** contributed to animal trial, sample and data collection, analyses and interpretation, figure organization and drafted the manuscript. **Mahmoud M. Abdelsattar** and **Yuze Fu** contributed to animal trial, sample collection and measurement. **Jianmin Chai** contributed to the conception, data analysis and interpretation, figure organization and manuscript writing. **Naifeng Zhang** contributed to the conception, project administration, supervision, draft editing. All authors have read and agreed to the published version of the manuscript.

## Data availability statement

The accession for the sequencing data in this study is NCBI Sequence Read Archive: # PRJNA851919 and PRJNA1068516.

## Declaration of competing interest

We declare that we have no financial and personal relationships with other people or organizations that can inappropriately influence our work, and there is no professional or other personal interest of any nature or kind in any product, service and/or company that could be construed as influencing the content of this paper.

## Acknowledgments

This study was funded by grants from National Natural Science Foundation of China (31872385), Foshan Postdoctoral Sustentation Fund (BKS209151), the Inner Mongolia Science and Technology Key Project (2021SZD0014), and the National Key R&D Program Projects (2018YFD0501902). The author thanks the goat farm for its cooperation in animal handling. We also appreciate Dr. Shiqin Wang from Anhui Science and Technology University, Prof. Shaoxian Cao, Dr. Hongbing Gui, Dr. Yue Wang, Dr. Xiaoxiao Guo and Dr. Han Zhang from Jiangsu Academy of Agricultural Sciences for their assistance in sampling collection.

## Appendix A. Supplementary data

Supplementary data to this article can be found online at https://doi.org/10.1016/j.aninu.2024.04.027.

## References

Abdelsattar MM, Zhuang Y, Cui K, Bi Y, Haridy M, Zhang N. Longitudinal investigations of anatomical and morphological development of the gastrointestinal tract in goats from colostrum to postweaning. J Dairy Sci 2022;105:2597–611.

AOAC. Official methods of analysis. 17th ed. Arlinton, VA: Association of Official Analytical Chemists; 2000.

Baldwin Vi RL, Liu M, Connor EE, Ramsay TG, Liu GE, Li CJ. Transcriptional reprogramming in rumen epithelium during the developmental transition of pre-ruminant to the ruminant in cattle. Animals (Basel) 2021;11:2870.

Beaumont M, Paes C, Mussard E, Knudsen C, Cauquil L, Aymard P, Barilly C, Gabinaud B, Zemb O, Fourre S, Gautier R, Lencina C, Eutamene H, Theodorou V, Canlet C, Combes S. Gut microbiota derived metabolites contribute to intestinal barrier maturation at the suckling-to-weaning transition. Gut Microb 2020;11:1268–86.

Chai J, Lv X, Diao Q, Usdrowski H, Zhuang Y, Huang W, Cui K, Zhang N. Solid diet manipulates rumen epithelial microbiota and its interactions with host transcriptomic in young ruminants. Environ Microbiol 2021;23:6557–68.

Chai J, Weiss CP, Beck PA, Zhao W, Li Y, Zhao J. Diet and monensin influence the temporal dynamics of the rumen microbiome in stocker and finishing cattle. J Anim Sci Biotechnol 2024a;15:12.

Chai J, Zhuang Y, Cui K, Bi Y, Zhang N. Metagenomics reveals the temporal dynamics of the rumen resistome and microbiome in goat kids. Microbiome 2024b;12:14.

Chang DH, Rhee MS, Jeong H, Kim S, Kim BCJGA. Draft genome sequence of acinetobacter sp. Hr7, isolated from hanwoo, Korean native cattle. Genome Announc 2015;3:e01358-14.

Chen L, Shen Y, Wang C, Ding L, Zhao F, Wang M, Fu J, Wang H. Megasphaera elsdenii lactate degradation pattern shifts in rumen acidosis models. Front Microbiol 2019;10:162.

Cheng CW, Biton M, Haber AL, Gunduz N, Eng G, Gaynor LT, Tripathi S, Calibasi-Kocal G, Rickelt S, Butty VL, Moreno-Serrano M, Iqbal AM, Bauer-Rowe KE, Imada S, Ulutas MS, Mylonas C, Whary MT, Levine SS, Basbinar Y, Hynes RO, Mino-Kenudson M, Deshpande V, Boyer LA, Fox JG, Terranova C, Rai K, Piwnica-Worms H, Mihaylova MM, Regev A, Yilmaz OH. Ketone body signaling mediates intestinal stem cell homeostasis and adaptation to diet. Cell 2019;178:1115–1131 e15.

Cole JR, Wang Q, Cardenas E, Fish J, Chai B, Farris RJ, Kulam-Syed-Mohideen AS, Mcgarrell DM, Marsh T, Garrity GM. The ribosomal database project: improved alignments and new tools for rrna analysis. Nucleic Acids Res 2009;37:D141–5.
Connor Ee BRT, Li Cj, Li Rw, Chung H. Gene expression in bovine rumen epithelium during weaning identifies molecular regulators of rumen development and growth. Funct Integr Genomics 2013;13(1):133–42.
Coutzac C, Jouniaux JM, Paci A, Schmidt J, Mallardo D, Seck A, Asvatourian V, Cassard L, Saulnier P, Lacroix L, Woerther PL, Vozy A, Naigeon M, Nebot-Bral L, Desbois M, Simeone E, Mateus C, Boselli L, Grivel J, Soularue E, Lepage P, Carbonnel F, Ascierto PA, Robert C, Chaput N. Systemic short chain fatty acids limit antitumor effect of ctla-4 blockade in hosts with cancer. Nat Commun 2020;11:2168.
Den Besten G, Bleeker A, Gerding A, Van Eunen K, Havinga R, Van Dijk TH, Oosterveer MH, Jonker JW, Groen AK, Reijngoud DJ, Bakker BM. Short-chain fatty acids protect against high-fat diet-induced obesity via a pparγ-dependent switch from lipogenesis to fat oxidation. Diabetes 2015;64:2398–408.
Furman O, Shenhav L, Sasson G, Kokou F, Honig H, Jacoby S, Hertz T, Cordero OX, Halperin E, Mizrahi I. Stochasticity constrained by deterministic effects of diet and age drive rumen microbiome assembly dynamics. Nat Commun 2020;11:1904.
Guo C, Sun D, Wang X, Mao S. A combined metabolomic and proteomic study revealed the difference in metabolite and protein expression profiles in ruminal tissue from goats fed hay or high-grain diets. Front Physiol 2019;10:66.
Han S, Van Treuren W, Fischer CR, Merrill BD, Defelice BC, Sanchez JM, Higginbottom SK, Guthrie L, Fall LA, Dodd D, Fischbach MA, Sonnenburg JL. A metabolomics pipeline for the mechanistic interrogation of the gut microbiome. Nature 2021;595:415–20.
Howell JJ, Manning BD. Mtor couples cellular nutrient sensing to organismal metabolic homeostasis. Trends Endocrinol Metab 2011;22:94–102.
Imhann F, Vich Vila A, Bonder MJ, Fu J, Gevers D, Visschedijk MC, Spekhorst LM, Alberts R, Franke L, Van Dullemen HM, Ter Steege RWF, Huttenhower C, Dijkstra G, Xavier RJ, Festen EaM, Wijmenga C, Zhernakova A, Weersma RK. Interplay of host genetics and gut microbiota underlying the onset and clinical presentation of inflammatory bowel disease. Gut 2018;67:108–19.
Jiao J, Wu J, Zhou C, He Z, Tan Z, Wang M. Ecological niches and assembly dynamics of diverse microbial consortia in the gastrointestine of goat kids. ISME J 2024;18:wrae002.
Kamke J, Kittelmann S, Soni P, Li Y, Tavendale M, Ganesh S, Janssen PH, Shi W, Froula J, Rubin EM, Attwood GT. Rumen metagenome and metatranscriptome analyses of low methane yield sheep reveals a sharpea-enriched microbiome characterised by lactic acid formation and utilisation. Microbiome 2016;4:56.
Karama M, Kambuyi K, Cenci-Goga BT, Malahlela M, Kalake A. Disease. Occurrence and antimicrobial resistance profiles of campylobacter jejuni , campylobacter coli , and campylobacter upsaliensis in beef cattle on cow–calf operations in South Africa. Foodb Pathog Dis 2020;17:440–6.
Kim CH. Control of lymphocyte functions by gut microbiota-derived short-chain fatty acids. Cell Mol Immunol 2021;18:1161–71.
Kirat D, Matsuda Y, Yamashiki N, Hayashi H, Kato S. Expression, cellular localization, and functional role of monocarboxylate transporter 4 (mct4) in the gastrointestinal tract of ruminants. Gene 2007;391:140–9.
Kozich JJ, Westcott SL, Baxter NT, Highlander SK, Schloss PD. Development of a dual-index sequencing strategy and curation pipeline for analyzing amplicon sequence data on the miseq illumina sequencing platform. Appl Environ Microbiol 2013;79:5112–20.
Lane MA, Baldwin RLT, Jesse BW. Sheep rumen metabolic development in response to age and dietary treatments. J Anim Sci 2000;78:1990–6.
Lane MA, Baldwin RLT, Jesse BW. Developmental changes in ketogenic enzyme gene expression during sheep rumen development. J Anim Sci 2002;80:1538–44.
Langfelder P, Horvath S. Wgcna: an r package for weighted correlation network analysis. BMC Bioinf 2008;9:559.
Li RW, Connor EE, Li C, Baldwin Vi RL, Sparks ME. Characterization of the rumen microbiota of pre-ruminant calves using metagenomic tools. Environ Microbiol 2012;14:129–39.
Li Z, Shen J, Xu Y, Zhu W. Metagenomic analysis reveals significant differences in microbiome and metabolic profiles in the rumen of sheep fed low n diet with increased urea supplementation. FEMS Microbiol Ecol 2020;96.
Lin L, Xie F, Sun D, Liu J, Zhu W, Mao S. Ruminal microbiome-host crosstalk stimulates the development of the ruminal epithelium in a lamb model. Microbiome 2019;7:83.
Liu X, Mao B, Gu J, Wu J, Cui S, Wang G, Zhao J, Zhang H, Chen W. Blautia-a new functional genus with potential probiotic properties? Gut Microb 2021;13:1–21.
Lv X, Chai J, Diao Q, Huang W, Zhuang Y, Zhang N. The signature microbiota drive rumen function shifts in goat kids introduced to solid diet regimes. Microorganisms 2019;7:516.
Malmuthuge N, Liang G, Guan LL. Regulation of rumen development in neonatal ruminants through microbial metagenomes and host transcriptomes. Genome Biol 2019;20:172.
Maus I, Tubbesing T, Wibberg D, Heyer R, Schlüter A. The role of petrimonas mucosa ing2-e5a t in mesophilic biogas reactor systems as deduced from multiomics analyses. Microorganisms 2020;8:2004.
Meale SJ, Li S, Azevedo P, Derakhshani H, Plaizier JC, Khafipour E, Steele MA. Development of ruminal and fecal microbiomes are affected by weaning but not weaning strategy in dairy calves. Front Microbiol 2016;7:582.
Meng C, Kuster B, Culhane AC, Gholami AM. A multivariate approach to the integration of multi-omics datasets. BMC Bioinf 2014;15:162.
Mizrahi I, Wallace RJ, Morais S. The rumen microbiome: balancing food security and environmental impacts. Nat Rev Microbiol 2021;19:553–66.
Moraïs S, Mizrahi I. The road not taken: the rumen microbiome, functional groups, and community states. Trends Microbiol 2019;27(6):538–49.
Naeem A, Drackley JK, Stamey J, Loor JJ. Role of metabolic and cellular proliferation genes in ruminal development in response to enhanced plane of nutrition in neonatal holstein calves. J Dairy Sci 2012;95:1807–20.
Okamoto T, Imaizumi K, Kaneko M. The role of tissue-specific ubiquitin ligases, rnf183, rnf186, rnf182 and rnf152, in disease and biological function. Int J Mol Sci 2020;21:3921.
Paillard D, Mckain N, Chaudhary LC, Walker ND, Pizette F, Koppova I, Mcewan NR, Kopecny J, Vercoe PE, Louis P, Wallace RJ. Relation between phylogenetic position, lipid metabolism and butyrate production by different butyrivibrio-like bacteria from the rumen. Antonie Leeuwenhoek 2007;91:417–22.
Salvi PS, Cowles RA. Butyrate and the intestinal epithelium: modulation of proliferation and inflammation in homeostasis and disease. Cells 2021;10:1775.
Sun D, Mao S, Zhu W, Liu J. Proteomic identification of ruminal epithelial protein expression profiles in response to starter feed supplementation in pre-weaned lambs. Anim Nutr 2021;7:1271–82.
Van Den Abbeele P, Belzer C, Goossens M, Kleerebezem M, De Vos WM, Thas O, De Weirdt R, Kerckhof FM, Van De Wiele T. Butyrate-producing clostridium cluster xiva species specifically colonize mucins in an in vitro gut model. ISME J 2013;7:949–61.
Van Soest PJ, Robertson JB, Lewis BA. Methods for dietary fiber, neutral detergent fiber, and nonstarch polysaccharides in relation to animal nutrition. J Dairy Sci 1991;74:3583–97.
Wang B, Rong X, Palladino E, Wang J, Fogelman AM, Martín M, Alrefai WA, Ford D, Tontonoz P. Phospholipid remodeling and cholesterol availability regulate intestinal stemness and tumorigenesis. Cell Stem Cell 2018;22:206–20.
Wang D, Chen L, Tang G, Yu J, Chen J, Li Z, Cao Y, Lei X, Deng L, Wu S, Guan LL, Yao J. Multi-omics revealed the long-term effect of ruminal keystone bacteria and the microbial metabolome on lactation performance in adult dairy goats. Microbiome 2023;11:215.
Wang Q, Zhou Y, Rychahou P, Fan TW, Lane AN, Weiss HL, Evers BM. Ketogenesis contributes to intestinal cell differentiation. Cell Death Differ 2017;24:458–68.
Wang W, Li C, Li F, Wang X, Zhang X, Liu T, Nian F, Yue X, Li F, Pan X, La Y, Mo F, Wang F, Li B. Effects of early feeding on the host rumen transcriptome and bacterial diversity in lambs. Sci Rep 2016;6:32479.
Wilson DF. Oxidative phosphorylation: regulation and role in cellular and tissue metabolism. J Physiol 2017;595:7023–38.
Wu M, Gu J, Guo R, Huang Y, Yang M. Structure of mammalian respiratory supercomplex i1iii2iv1. Cell 2016;167:1598–1609.e10.
Xue MY, Sun HZ, Wu XH, Liu JX, Guan LL. Multi-omics reveals that the rumen microbiome and its metabolome together with the host metabolome contribute to individualized dairy cow performance. Microbiome 2020a;8:64.
Xue Y, Lin L, Hu F, Zhu W, Mao S. Disruption of ruminal homeostasis by malnutrition involved in systemic ruminal microbiota-host interactions in a pregnant sheep model. Microbiome 2020b;8:138.
Yin X, Ji S, Duan C, Tian P, Ju S, Yan H, Zhang Y, Liu Y. Age-related changes in the ruminal microbiota and their relationship with rumen fermentation in lambs. Front Microbiol 2021;12:679135.
Yohe TT, Schramm H, White RR, Hanigan MD, Parsons CLM, Tucker HLM, Enger BD, Hardy NR, Daniels KM. Form of calf diet and the rumen. Ii: impact on volatile fatty acid absorption. J Dairy Sci 2019;102:8502–12.
Yu G, Xu C, Zhang D, Ju F, Ni Y. Metorigin: discriminating the origins of microbial metabolites for integrative analysis of the gut microbiome and metabolome. iMeta 2022;1:e10.
Zhang C, Luo X, Chen J, Zhou B, Yang G. Osteoprotegerin promotes liver steatosis by targeting the erk-pparγ-cd36 pathway. Diabetes 2019;68:db181055.
Zhang Y, Cai W, Li Q, Wang Y, Wang Z, Zhang Q, Xu L, Xu L, Hu X, Zhu B, Gao X, Chen Y, Gao H, Li J, Zhang L. Transcriptome analysis of bovine rumen tissue in three developmental stages. Front Genet 2022;13:821406.
Zhao C, Bao L, Qiu M, Wu K, Zhao Y, Feng L, Xiang K, Zhang N, Hu X, Fu Y. Commensal cow roseburia reduces gut-dysbiosis-induced mastitis through inhibiting bacterial translocation by producing butyrate in mice. Cell Rep 2022;41:111681.
Zhuang Y, Chai J, Abdelsattar MM, Fu Y, Zhang N. Transcriptomic and metabolomic insights into the roles of exogenous β-hydroxybutyrate acid for the development of rumen epithelium in young goats. Anim Nutr 2023a;15:10–21.
Zhuang Y, Lv X, Cui K, Chai J, Zhang N. Early solid diet supplementation influences the proteomics of rumen epithelium in goat kids. Biology 2023b;12:684.